**The EMBO Journal** Vol. 20 No. 9 pp. 2140–2151, 2001

# The tripartite motif family identifies cell compartments

**Alexandre Reymond[1,2], Germana Meroni[1,3], Anna Fantozzi[4,5], Giuseppe Merla[1,3], Stefano Cairo[1,3], Lucilla Luzi[4,5], Daniela Riganelli[4], Elena Zanaria[1], Silvia Messali[1], Silvia Cainarca[1], Alessandro Guffanti[1], Saverio Minucci[5], Pier Giuseppe Pelicci[4,5,6] and Andrea Ballabio[1,3,6,7]**

[1]Telethon Institute of Genetics and Medicine (TIGEM), San Raffaele Biomedical Science Park, Milan, [4]Internal Medicine and Oncological Sciences Institute, Perugia University, 06100 Perugia, [5]Department of Experimental Oncology, European Institute of Oncology (IEO), 20141 Milan and [7]Università Vita e Salute, San Raffaele Biomedical Science Park, Milan, Italy

[2]Present address: Division of Medical Genetics, Geneva University Medical School, 1 rue Michel Servet, 1211 Geneva 4, Switzerland
[3]Present address: TIGEM, Via Pietro Castellino 111, 80131 Naples, Italy

[6]Corresponding authors at: TIGEM, Via Pietro Castellino 111, 80131 Naples or Department of Experimental Oncology, European Institute of Oncology (IEO), Via Ripamonti 435, 20141 Milan, Italy
e-mail: ballabio@tigem.it or pgpelicci@ieo.it

A.Reymond and G.Meroni contributed equally to this work

**A functional genomic approach, based on systematic data gathering, was used to characterize a family of proteins containing a tripartite motif (TRIM). A total of 37 TRIM genes/proteins were studied, 21 of which were novel. The results demonstrate that TRIM proteins share a common function: by means of homo-multimerization they identify specific cell compartments.**

*Keywords*: cell compartmentalization/functional genomics/nuclear bodies/RBCC/tripartite motif

## Introduction

The complete or partial sequence information on the genomes of several organisms is now available (Goffeau *et al*., 1996; Blattner *et al*., 1997; The *C. elegans* Sequencing Consortium, 1998; Dunham *et al*., 1999; Adams *et al*., 2000; The Chromosome 21 Mapping and Sequencing Consortium, 2000). This information allows the study of molecular mechanisms at the level of large numbers of genes, thus modifying the way biological questions are addressed. Large-scale surveys of protein contents, protein subcellular localization and of potential interacting partners have, indeed, provided relevant functional information (Shevchenko *et al*., 1996; Martzen *et al*., 1999; Ross-Macdonald *et al*., 1999; Brent, 2000; Uetz *et al*., 2000; Walhout *et al*., 2000). Such systematic data gathering on a protein family may provide further information towards the assignment of function to homologous protein sequences.

We tested this postulate on the emerging tripartite motif (TRIM) protein family (also known as the RBCC family) (Reddy *et al*., 1992; Borden, 1998). The TRIM is composed of three zinc-binding domains, a RING (R), a B-box type 1 (B1) and a B-box type 2 (B2), followed by a coiled-coil (CC) region (Reddy *et al*., 1992; Borden, 1998). Genes belonging to this family are implicated in a variety of processes, such as development and cell growth, and are involved in several human diseases. PYRIN/MARENOSTRIN, MID1 and MUL are mutated in familial Mediterranean fever, X-linked Opitz/GBBB syndrome and mulibrey nanism, respectively (Quaderi *et al*., 1997; The French FMF Consortium, 1997; The International FMF Consortium 1997; Avela *et al*., 2000), whereas PML, RFP and Tif1 acquire oncogenic activity when fused to RARα, RET or B-raf, respectively (Takahashi *et al*., 1988; Grignani *et al*., 1994; Le Douarin *et al*., 1995).

Very little is known about the biological and molecular mechanisms mediated by the TRIM genes (Friedman *et al*., 1996; Kim *et al*., 1996; Le Douarin *et al*., 1996; Moosmann *et al*., 1996; Quignon *et al*., 1998; Wang *et al*., 1998; Nielsen *et al*., 1999; Pearson *et al*., 2000; Zhong *et al*., 2000b). To tackle this issue, we devised a strategy based on a bioinformatic approach combined with systematic functional data gathering (Figure 1). The collected data are summarized in Table I and are accessible through our web page (www.tigem.it/TRIM). The pertinence of this approach is demonstrated by the identification of a common molecular property shared by TRIM proteins.

## Results

### *The TRIM family*

To identify TRIM family members, we first screened the dbEST databases using a consensus of the B-box domain. We identified a total of 37 TRIM members in mammals (TRIM1–37), 21 of which were previously undescribed (TRIM1–17 and 34–37). In addition, we found 34 new alternative splice forms and a TRIM expressed pseudogene ψ (Figure 2A). Eighty-one sequences have been deposited in the DDBJ/EMBL/GenBank database.

These extensive data allowed us to define the sequence patterns of the TRIM-specific RING domain and the consensi of the B1 and B2 domains (Figure 2B). The B1 and B2 domains have different lengths and consensi and, when found together, the type 1 B-box always precedes the type 2. A predicted CC region invariably follows (Figure 2). The B-boxes appear to be critical determinants of the TRIM motif, since, at variance with the R and CC domains, they were only found within this protein family. The C-terminal portion of these proteins may contain known domains, such as the RFP-like (B30.2), the

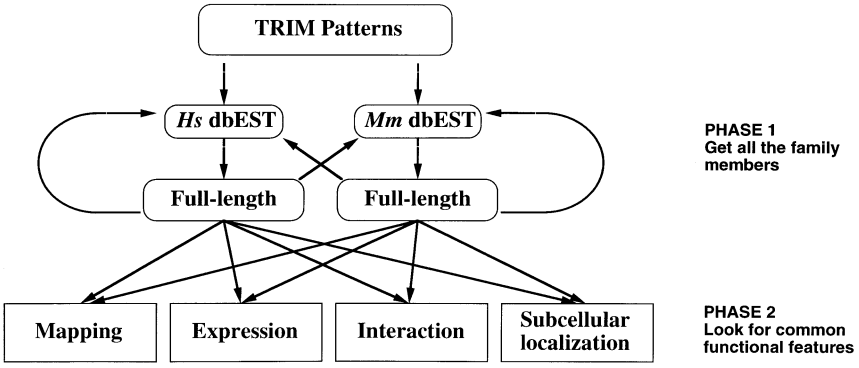


**Fig. 1.** Schematic outline of the strategy used in the first phase to identify and clone full-length TRIM cDNAs and in the second phase to find common functional features through systematic data gathering. *Hs*, *Homo sapiens*; *Mm*, *Mus musculus*.

NHL, the TSS-PHD-BROMO, the ARF or uncharacterized sequences (Figure 2A) (Vitale *et al*., 1996; Cao *et al*., 1997; Slack and Ruvkun, 1998; Venturini *et al*., 1999).

We found that while some of the above-defined domains can be present or absent, their order from the N- to the C-terminal end of the protein is always maintained (R-B1-B2-CC-Cterm; see Figure 2A). Notably, this arrangement is conserved throughout evolution, further supporting its functional relevance (Bellini *et al*., 1995; Shou *et al*., 1996; Frank and Roth, 1998; Slack *et al*., 2000). These features suggest that the TRIM may serve as an integrated functional structure, rather than a collection of separate modules.

To study the evolutionary history of the TRIM gene family, we determined their chromosomal localization (Table I). The TRIM genes are dispersed throughout the genome, with the exception of two clusters located in the HLA region in 6p21–23 (TRIM10, 15, 26, 27 and 31) and 11p15 (TRIM5, 6, 21, 22, 34 and TRIMψ). The RH raw data and a schematic representation of the clusters can be accessed through our web page (www.tigem.it/TRIM). With the exception of TRIM31, the genes within the 6p21–23 and 11p15 clusters share the same R, B2, CC and RFP-like domain composition. Interestingly, in the HLA chromosomal region this conserved C-terminal domain is also present in the butyrophilin gene, which encodes an unrelated protein lacking the TRIM (Henry *et al*., 1998). In contrast, TRIM3, distally located on chromosome 11p arm, lacks the RFP-like domain and contains an NHL domain at the C-terminus of the predicted protein product. Sequence comparison of RFP-like domains shows that TRIM genes within each cluster are more similar to each other than to other members of the family (data not shown). This observation is compatible with possible recent duplications of ancestor TRIM genes in these regions.

We performed systematic expression analysis of TRIM genes by both northern blotting and RNA *in situ* hybridization using adult and embryonic mouse tissues. The results revealed heterogeneous expression patterns among the TRIM genes, thereby suggesting independent evolution of their regulatory regions. A short description of the expression patterns for each of the TRIM genes is presented in Table I and the RNA *in situ* hybridization data of 22 TRIM genes are accessible through our web site (www.tigem.it/TRIM). Two examples of the expression of TRIM genes during development are presented in Figure 3.

### *TRIM proteins homo-multimerize through their CC region*

We investigated whether the common structural traits of the TRIM translate into shared functional features. The presence of a CC region strongly suggested the possibility of cross-interaction among TRIM proteins (Lupas, 1996). To investigate TRIM protein homo- and hetero-dimerization properties, we took advantage of the interaction-mating technique, an extension of the two-hybrid system. Consistent with previous work, we confirmed the homo-interaction of TRIM18 (MID1) and 27 (RFP) (see Figure 4I) (Cao *et al*., 1997; Cainarca *et al*., 1999). Similarly, TRIM1, 3, 5, 6, 8, 9, 10, 11, 21, 23, 24, 25, 26, 29, 31 and 32 were shown to homo-interact. Heterologous interaction, instead, is uncommon among family members and only a few putative interologs were mapped (Figure 4I). The ability of TRIM6, 8, 11, 23, 28, 29 and 30 to homo-interact was confirmed by *in vitro* and/or *in vivo* co-immunoprecipitation experiments (Table I; Figure 5I) (Reymond and Brent, 1995). Notably, TRIM28 and 30, which scored negative in the two-hybrid screen, were shown to homo-interact both *in vivo* and *in vitro*.

To map the structural determinants responsible for their self-association, we generated TRIM mutants carrying individual deletions of relevant protein regions [R, B-boxes (BB), CC, RFP-like, and N- or C-terminal regions; Figure 5A] and analyzed them by interaction mating and *in vivo* co-immunoprecipitation. Deletion of the CC region resulted in the loss of self-association, while deletion of the other regions only partially affected binding (Figure 5B–D, F and I). Isolated CC, but not isolated R or BB, was able to self-associate, suggesting that the CC region is necessary and sufficient for homo-interaction (Figure 5E).

Given the strong self-association properties found for essentially all of the TRIM proteins, we hypothesized that their CC region mediates the formation of higher order complexes. We tested this assumption using gel filtration analysis of *in vitro* translated TRIM proteins. Each tested TRIM protein (TRIM6, 8, 11, 23, 28, 29 and 30) eluted in fractions corresponding to high molecular weight complexes (Figures 4J, 5G and H). Comparable results were obtained using cell lysates overexpressing TRIM proteins

(not shown). Similar results were previously gathered for TRIM18 (MID1), 19 (PML) and 28 (TIF1β) (Cainarca *et al*., 1999; Grignani *et al*., 1999; Minucci *et al*., 2000; Peng *et al*., 2000). Gel filtration analysis of the various TRIM deletion mutants indicated the critical involvement of the CC region in the formation of high molecular weight complexes. Wild-type TRIM proteins elute as multimeric complexes, while the ΔCC mutant proteins elute in fractions corresponding to monomers. In contrast, deletions of either BB, R or RFP did not affect the formation of high molecular weight complexes (Figure 5G and H). Together, these results suggest that the diverse TRIM proteins form high molecular weight complexes *in vivo* as a consequence of the self-association properties of their CC regions.

### *TRIM proteins identify cell compartments*

A few TRIM proteins have been previously characterized for their subcellular localization and shown to be associated with specific compartments, such as nuclear bodies (PML/TRIM19, TIF1/TRIM24 and RFP/TRIM27) or the microtubules (MID1/TRIM18 and MID2/TRIM1) (Dyck *et al*., 1994; Le Douarin *et al*., 1995; Cao *et al*., 1998; Buchner *et al*., 1999; Cainarca *et al*., 1999; Schweiger *et al*., 1999; Zhong *et al*., 2000b). We therefore investigated the subcellular localization of all TRIM proteins in living cells using green fluorescent protein (GFP) technology. Results are summarized in Table I and are accessible through our web links (www.tigem.it/TRIM). The great majority of TRIM proteins localize to discrete cytoplasmic or nuclear structures sometimes associated with a diffusely stained background. In the case of cytoplasmic TRIM proteins, these putative structural domains are associated with filaments (TRIM1, 2, 3 and 18; Figure 4C), or assume a cytoplasmic ribbon-like structure (TRIM29; Figure 4A). Other TRIM proteins are concentrated in 'cytoplasmic bodies' of variable size (TRIM4, 5, 6, 9, 10, 12, 14, 21, 22, 23, 26, 27, 30 and 32; Figure 4B, D and H), occasionally located around the nucleus (TRIM13; Figure 4F). Nuclear TRIM proteins localize to structures best described as 'nuclear bodies' (TRIM8, 19, 30 and 32; Figure 4E) or 'nuclear sticks' (TRIM6). The members of the bromodomain-containing subfamily (TRIM24, 28 and 33) associate with specific chromatin regions, consistent with the proposed role of this domain (Figure 4G) (Jacobson *et al*., 2000).

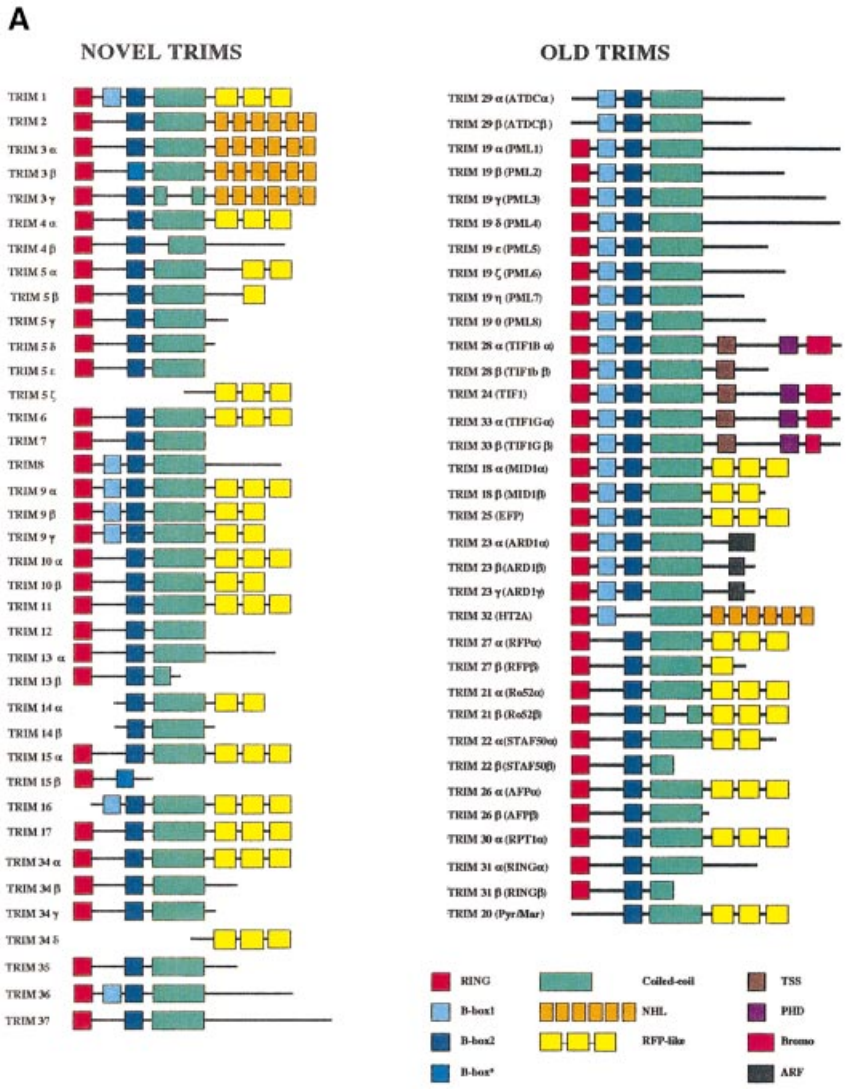

To define better the compartments identified by TRIM proteins, we performed co-localization studies using compartment-specific markers. U2OS cells were transiently transfected with the multiple GFP–TRIM fusion constructs and the green fluorescent signals were compared with distinct compartments outlined by specific antibodies. Based on the TRIM localization pattern observed (cytoplasmic speckled, nuclear speckled, filamentous, etc.; see above), co-localization experiments were performed with markers of the Golgi apparatus, endocytic vesicles,

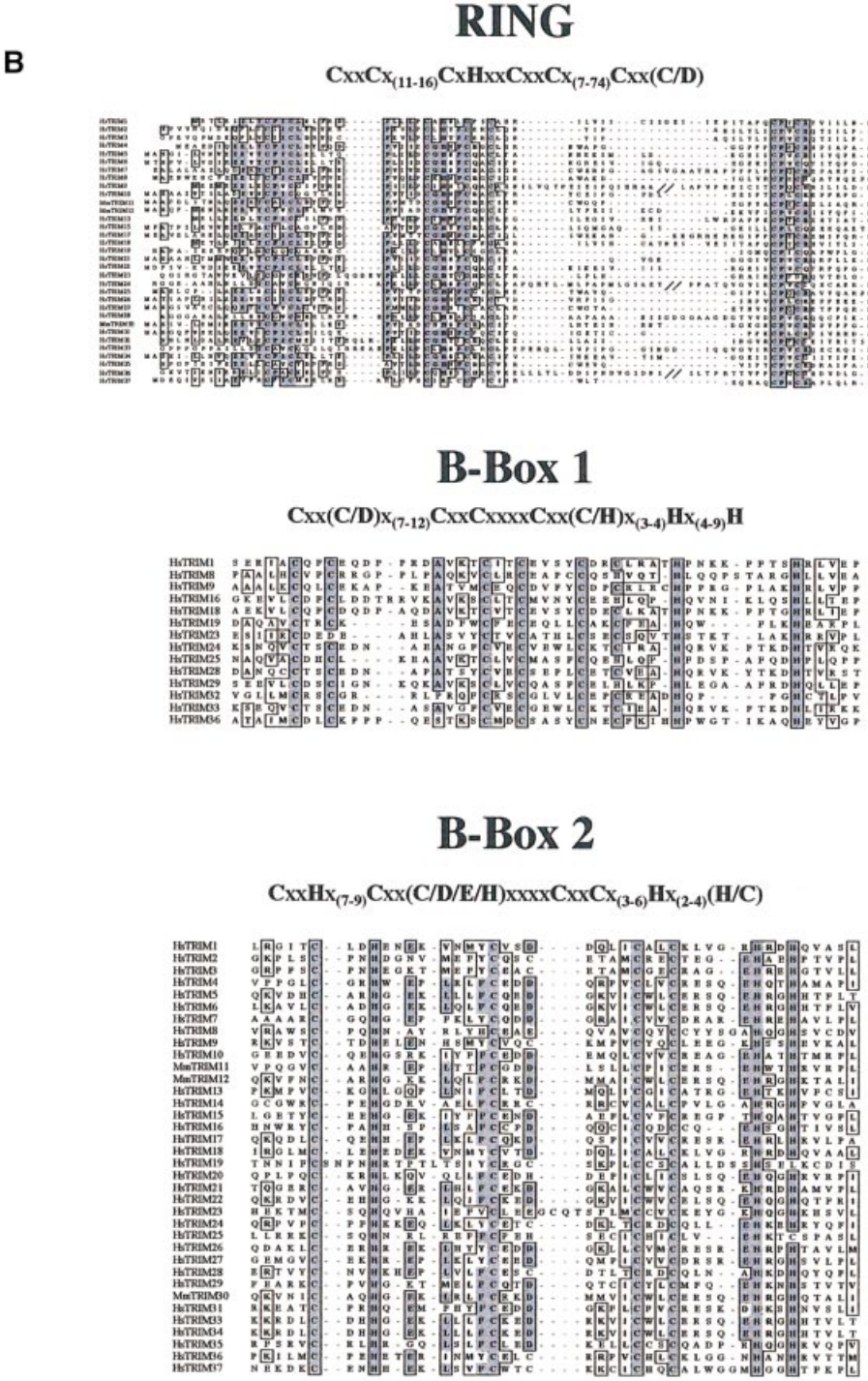


**Fig. 2.** The TRIM protein family. (**A**) Schematic representation of the TRIM proteins identified in the screen described in Figure 1. Color coding is as follows: red squares, RING domain; light blue squares, B-box type 1 domain; dark blue squares, B-box type 2 domain; marine blue squares, B-box of TRIM alternatively spliced isoforms not following type 1 or 2 criteria; green rectangles, CC region; orange rectangles, NHL repeats domain; yellow rectangles, RFP-like domain regions; brown squares, TSS domain; purple squares, PHD domain; magenta rectangles, bromodomain; black squares, ARF domain. (**B**) Alignments of the RING, the B-box type 1 and the B-box type 2 domains. The consensus sequences are indicated above. Conserved and similar amino acids are boxed. TRIM9, 24 and 36 double backslashes indicate a discontinuity in the sequence. Abbreviations are as in Figure 1. R, B1 and B2 consensi were built with 33, 14 and 35 mammalian sequences, respectively. Orthologous sequences were omitted for obvious reasons. Please note that TRIM37 in the R domain and TRIM19 and 23 in the B2 domain do not respect the spacing between conserved residues.

**Table I.** The tripartite motif family

| Name[a] | | Domains[b] | Isoforms[c] | Mapping[d] | Adult expression[e] | Embryonic expression[e] | Homodimerization[f] | | | Cellular localization[g] |
|---|---|---|---|---|---|---|---|---|---|---|
| | | | | | | | IM | IVT | IV | |
| TRIM1 | MID2 | R B1 B2 CC RFP | | Xq22–25 (RH) | ubiquitous | heart, kidney, CNS, thymus, eye | + | | | filamentous (C) |
| TRIM2 | | R B2 CC NHL | | 4q27–q34 (RH) | brain, kidney, pancreas, spleen (7.5 kb) | CNS, gut, retina, lung, kidney | – | | | filamentous (C) |
| TRIM3 | | R B2 CC NHL | 3 | 11p15 (RH) | heart, brain, liver, pancreas (4 + 3 kb) | CNS, eye, kidney, lung | + | | | diffuse (C) |
| TRIM4 | | R B2 CC RFP | 2 | 7q22 (RH) | ubiquitous (3 kb) | | – | | | speckles (C) |
| TRIM5 | | R B2 CC RFP | 5 | 11p15 (RH) | ubiquitous (*) | | + | | | speckles (C) |
| TRIM6 | | R B2 CC RFP | | 11p15 (RH) | ubiquitous (*) | ubiquitous | + | + | | speckles (C) |
| TRIM7 | | R B2 CC | | 5qter (RH) | sk. muscle (2 kb) | ubiquitous | – | | | diffuse (N and C) |
| TRIM8 | | R B1 B2 CC | | 10q24 (RH) | ubiquitous (3 kb) | CNS, kidney, lens, gut | + | + | + | speckles (N) |
| TRIM9 | | R B1 B2 CC RFP | 3 | 14q21–24 (RH) | brain (4.4 kb) | CNS | + | | | speckles (C) |
| TRIM10 | HERF1 | R B2 CC RFP | 2 | 6p21–23 (RH) | kidney, colon, liver (4.4 kb) | liver | + | | | aggregates (C) |
| TRIM11 | | R B2 CC RFP | | 1q32–44 (RH) | ubiquitous (*) | CNS, kidney, thymus, gut | + | | + | diffuse (N and C) |
| TRIM12 | | R B2 CC | | | liver (4.4 kb, Mm) | CNS, liver, kidney, olfactory epithelium | – | | | diffuse, speckles (C) |
| TRIM13 | LEU5 | R B2 CC | 2 | 13q14 (RH) | testis, heart, sk. muscle (1.8 kb) | CNS, kidney, adrenal primordium | – | | | speckles (C) |
| TRIM14 | | B2 CC RFP | 2 | 9q22–31 (RH) | ubiquitous (5 kb) | | – | | | speckles (C) |
| TRIM15 | | R B2 CC RFP | 2 | 6p21–23 (RH) | | | | | | |
| TRIM16 | EBBP | B2 CC RFP | | 17p11.2 (RH) | | skeletal muscle system | | | | |
| TRIM17 | TERF | R B2 CC RFP | | 1q42 (RH) | | ubiquitous | | | | |
| TRIM18 | MID1 | R B1 B2 CC RFP | 2 | Xp22.3 | ubiquitous (5 kb) | CNS, gastrointestinal tract | + | | | filamentous (C) |
| TRIM19 | PML | R B1 B2 CC | 11 | 15q22–24 | ubiquitous (3 kb) | CNS, ubiquitous | – | | | bodies (N) |
| TRIM20 | PYRIN | B2 CC RFP | | 16p13.3 | | | – | | | diffuse (C) |
| TRIM21 | SSA/RO | R B2 CC RFP | 2 | 11p15 (RH) | ubiquitous (2.2 kb) | CNS, ubiquitous | + | | | diffuse, speckles (C) |
| TRIM22 | STAF50 | R B2 CC RFP | | 11p15 (RH) | ubiquitous (4.5 + 3.5 kb) | | – | | | diffuse, speckles (C) |
| TRIM23 | ARD1 | R B1 B2 CC ARF | 3 | 5q11–14 (RH) | heart, brain, testis, others (4 kb) | low ubiquitous expression | + | + | | speckles (N and C) |
| TRIM24 | TIF | R B1 B2 CC BROMO | | 7q33–35 (RH) | testis (4.2 kb) | CNS, eye, urogenital system | + | | | speckles (C) |
| TRIM25 | EFP | R B1 B2 CC RFP | | 17q21–23 (RH) | placenta, ubiquitous (7 kb) | liver | + | | | diffuse, aggregates (C) |
| TRIM26 | AFP | R B2 CC RFP | 2 | 6p21–23 (RH) | prostate, ovary, testis (6 kb) | | + | | | diffuse (C) |
| TRIM27 | RFP | R B2 CC RFP | 2 | 6p21–23 (RH) | | ubiquitous | – | | | speckles (C) |
| TRIM28 | TIF1β | R B1 B2 CC BROMO | 2 | 19qter (RH) | ubiquitous (4.5 + 3 kb) | ubiquitous | – | + | + | chromatin domains (N) |
| TRIM29 | ATDC | B1 B2 CC | 2 | 11q22–23 (RH) | placenta, prostate, thymus (3 kb) | external ectodermal layer | + | + | | filamentous (C) |
| TRIM30 | RPT1 | R B2 CC RFP | 2 | | spleen (4 kb, Mm) | | – | + | + | speckles (N and C) |
| TRIM31 | RING | R B2 CC | 2 | 6p21–23 | | | + | | | diffuse (N and C) |
| TRIM32 | HT2A | R B1 CC NHL | | 9q32–33 (RH) | testis, heart, sk. muscle (3.5 kb) | ubiquitous | + | | | diffuse and speckled (C) |
| TRIM33 | TIF1γ | R B1 B2 CC BROMO | 2 | 1p13 | | | | | | |
| TRIM34 | | R B2 CC RFP | 6 | 11p15 (RH) | | | | | | |
| TRIM35 | | R B2 CC | | chr4 | | | | | | |
| TRIM36 | | R B1 B2 CC | | 5q22 | | | | | | |
| TRIM37 | MUL | R B2 CC | | 17q22–23 | | | | | | |
| Pseudogene ψ | | | | 11p15 | | | | | | |

An interactive version of this table with links to the accession numbers, the mapping, the RNA *in situ* and subcellular localization data is accessible at http://www.tigem.it/TRIM.

[a]Commonly used names of the already published TRIM proteins are reported in the second column. During the preparation of this manuscript, some of the novel TRIM genes we characterized have been independently isolated; their names are also reported.

[b]In this case the BROMO acronym should be understood as TSS-PHD-BROMO domain.

[c]The number of alternatively spliced forms is indicated.

[d]RH, radiation hybrid mapping performed to determine chromosomal localization.

[e]Tissues showing a high level of expression are underlined; (*), smeary signal; the approximate size of the transcript is in parentheses; Mm, analysis performed on mouse tissues.

[f]Homodimerization determined by interaction mating (IM), *in vitro* co-immunoprecipitation (IVT) and *in vivo* co-immunoprecipitation (IV).

[g]Cellular localization determined in HeLa and U2OS cells. C, cytoplasm; N, nucleus.

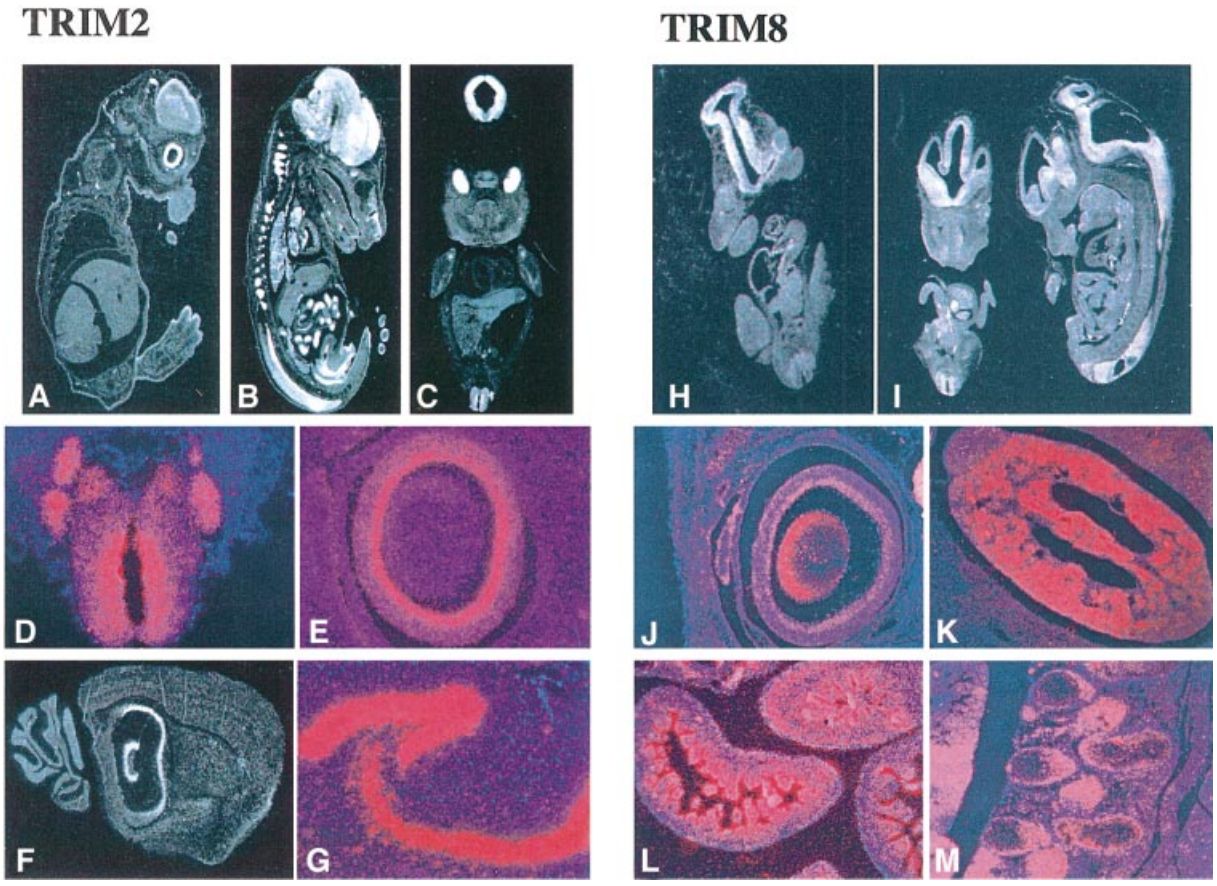


**Fig. 3.** TRIM expression pattern during mouse embryonic development. TRIM2 is preferentially expressed in the central nervous system and gut. (**A** and **B**) Sagittal sections of E12.5 and E14.5 embryos, respectively. (**C**) A coronal section of an E12.5 embryo. All three panels reveal high expression of TRIM2 in the nervous system (in particular in the telencephalon, cranial and dorsal root ganglia, and eye) and in the gut (midgut and duodenum). Higher magnification panels highlight expression of TRIM2 in the neural tube and in the dorsal root ganglia (**D**) and in the inner neural layer of the retina (**E**). (**F** and **G**) Expression in the adult brain, particularly high in the hippocampus. TRIM8 is mainly expressed in the kidney, gut and central nervous system. Coronal and sagittal sections of E10.5 and E12.5 embryos (**H** and **I**) show expression in the central nervous system. The higher magnification panels show a high level of expression at the E14.5 stage in: the eye (lens and inner neural layer of the retina) (**J**); the primitive glomeruli of the developing kidney (**K**); the villi of the gut (**L**); and the dorsal root ganglia (**M**).

clathrin-coated pits, mitochondria, coil bodies, PML-specific nuclear bodies, spliceosomes, BRCA-1-specific nuclear bodies, intermediate filaments, tubulin and actin. The experiments are summarized in Table II and the images can be visualized through our web site (www.tigem.it/TRIM). The results show that, with the exception of MID2/TRIM1 and MID1/TRIM18, none of the TRIM proteins co-localizes with the tested structures. Furthermore, an internalization assay showed that the investigated TRIM proteins do not co-localize with rhodamine-conjugated transferrin, a marker for recycling endosomes. Therefore, our studies strongly suggest that most of the TRIM proteins define novel subcellular compartments.

Disruption of the TRIM CC region was always associated with diffuse localization (see, for example, the ΔCC TRIM6, 8 and 29 mutants; Figure 6). In contrast, independent deletions of R or BB induced relocalization of the mutant protein to aberrant cellular structures (Figure 6). For example, deletion of the R domain in TRIM6 and 8, or of the entire BB region in TRIM 6 and 29, causes formation of new structures, different in shape, size and number from those observed with the full-length protein. Deletion of the B1 domain in an R-B1-B2-CC-type TRIM was indeed sufficient to alter—although less dramatically—subcellular localization (Figure 6), indicating that the integrity of the TRIM is absolutely required for proper subcellular localization of TRIM proteins. The contribution of other regions of the TRIM proteins, instead, varies from protein to protein. Deletion of the C-terminal region of TRIM6 had no effect, while a similar deletion in TRIM8 and TRIM29 resulted in protein mislocalization (Figure 6). The importance of the RFP-like domain in proper localization of TRIM18 (MID1) has been demonstrated in Opitz syndrome (Cainarca *et al*., 1999; Schweiger *et al*., 1999).

Together, these results suggest that TRIM proteins define a variety of different cellular compartments as a consequence of their propensity to form high-order molecular weight structures. In particular, it appears that the CC region of the TRIM is indispensable for the formation of high molecular weight complexes and cellular compartments, while the R and B-boxes (and in given examples other domains) cooperate for proper subcellular localization.

Some of the artificially created deletion mutants mimic naturally occurring TRIM alternatively spliced isoforms (Figures 2A and 5A). TRIM21β, for example, lacks the CC region, does not homodimerize and presents a diffuse

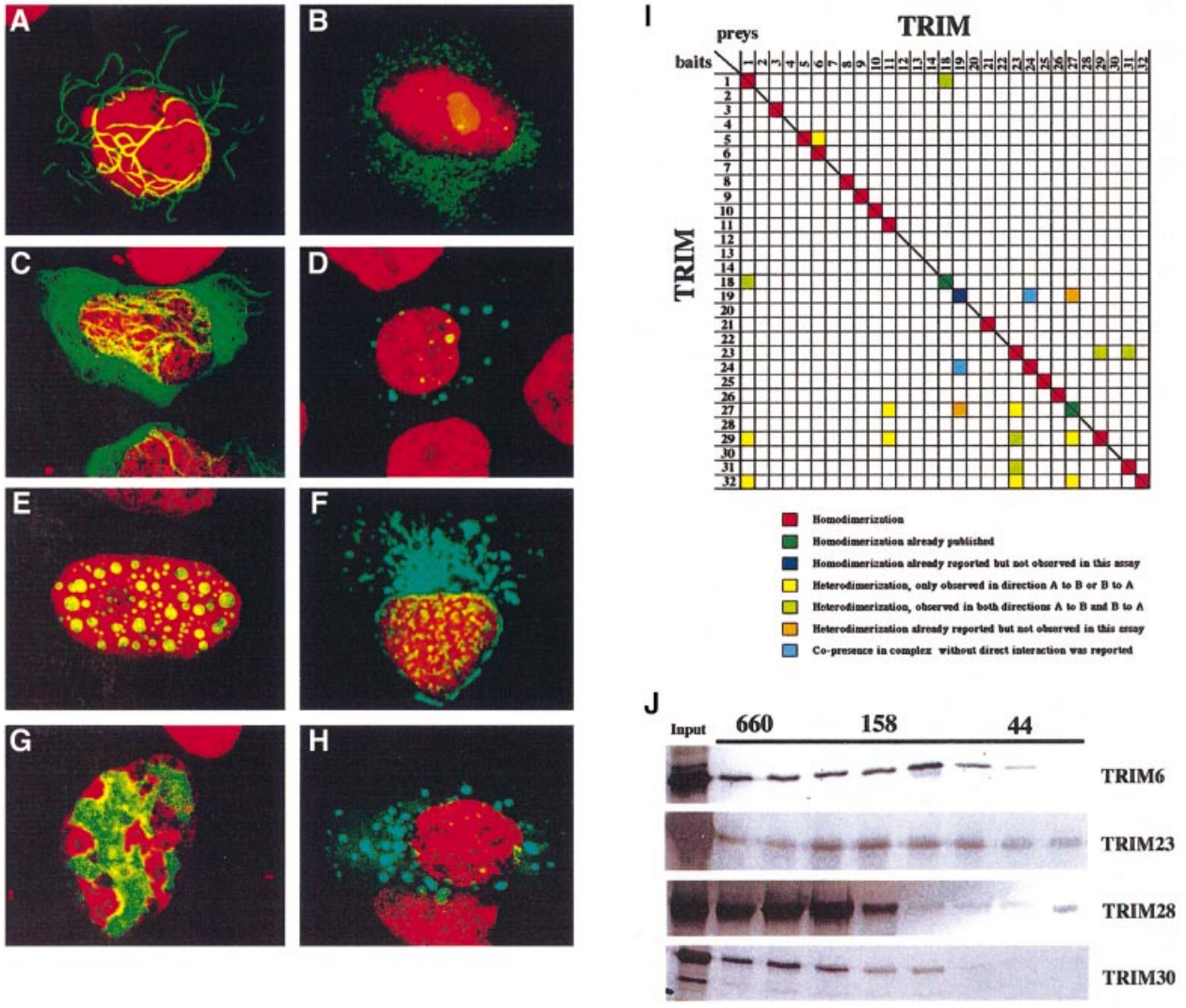


**Fig. 4.** TRIM proteins homomultimerize and associate with specific subcellular structures. Subcellular localization of TRIM29 (**A**), TRIM4 (**B**), TRIM2 (**C**), TRIM5 (**D**), TRIM8 (**E**), TRIM13 (**F**), TRIM28 (**G**) and TRIM9 (**H**). U2OS and HeLa cells were transfected with plasmids encoding EGFP–TRIM fusions. All TRIM proteins localized to particular subcellular compartments: TRIM29, to cytoplasmic ribbon-like structures; TRIM2, to cytoplasmic filaments; TRIM4, 5 and 9, to 'cytoplasmic bodies'; TRIM8, to specific nuclear bodies; TRIM13, around the nucleus; and TRIM28, to specific chromatin regions. (**I**) Interaction-mating matrix of 32 TRIM ORFs fused to the LexA binding domain (bait) or to the B42-SV40 NLS-HA-tag domains (preys). Color coding is as follows: red squares, homodimerization; dark green squares, homodimerization previously reported and detected in the present assay; dark blue squares, homodimerization previously reported and not detected in the present assay; yellow squares, heterodimerization detected in either bait-X/prey-Y or bait-Y/prey-X orientation; light green squares, heterodimerization detected in both bait-X/prey-Y and bait-Y/prey-X orientations; orange squares, heterodimerization previously reported and not detected in either bait-X/prey-Y or bait-Y/prey-X orientation; light blue squares, co-presence without direct interaction in a protein complex reported (Grignani *et al*., 1996; Cao *et al*., 1997, 1998; Cainarca *et al*., 1999; Zhong *et al*., 1999a). (**J**) Superose 6 gel filtration of *in vitro* translated TRIM6, 23, 28 and 30 proteins. Their elution peaks correspond to formation of homomultimeric complexes. Elution of proteins of known molecular weight (kDa) is indicated above.

nuclear and cytoplasmic localization pattern, while the longer R-B2-CC-RFP isoform (TRIM21α) is capable of homodimerization and concentrates in discrete cytoplasmic speckles (Figure 5F; Table I; www.tigem.it/TRIM). Likewise, upon co-expression, the shorter TRIM30β isoform was shown to displace the α isoform from the cytoplasmic bodies it identifies (G.Merla and A.Reymond, in preparation). Moreover, deletion of the BB or the C-terminal domain of TRIM11, one of the few diffuse TRIM proteins, confers a compartmentalized pattern to the protein (www.tigem.it/TRIM). These data allow us to speculate on an even more subtle involvement of the TRIM proteins and their alternatively spliced isoforms in the regulation of compartmentalization.

## Discussion

Nature often uses the same structures to perform functions that are similar at the biochemical level, but might be very different in a physiological context. This effective and 'economical' way of handling functions is achieved by duplicating structures, hence generating gene families. The analysis of the entire human genome is expanding both the number and size of such families, creating the need to develop new approaches to identify the functional properties of their members. Towards this goal, we implemented a combinatorial strategy. After definition of a protein family with *in silico* and classical molecular biology approaches, we systematically investigated the

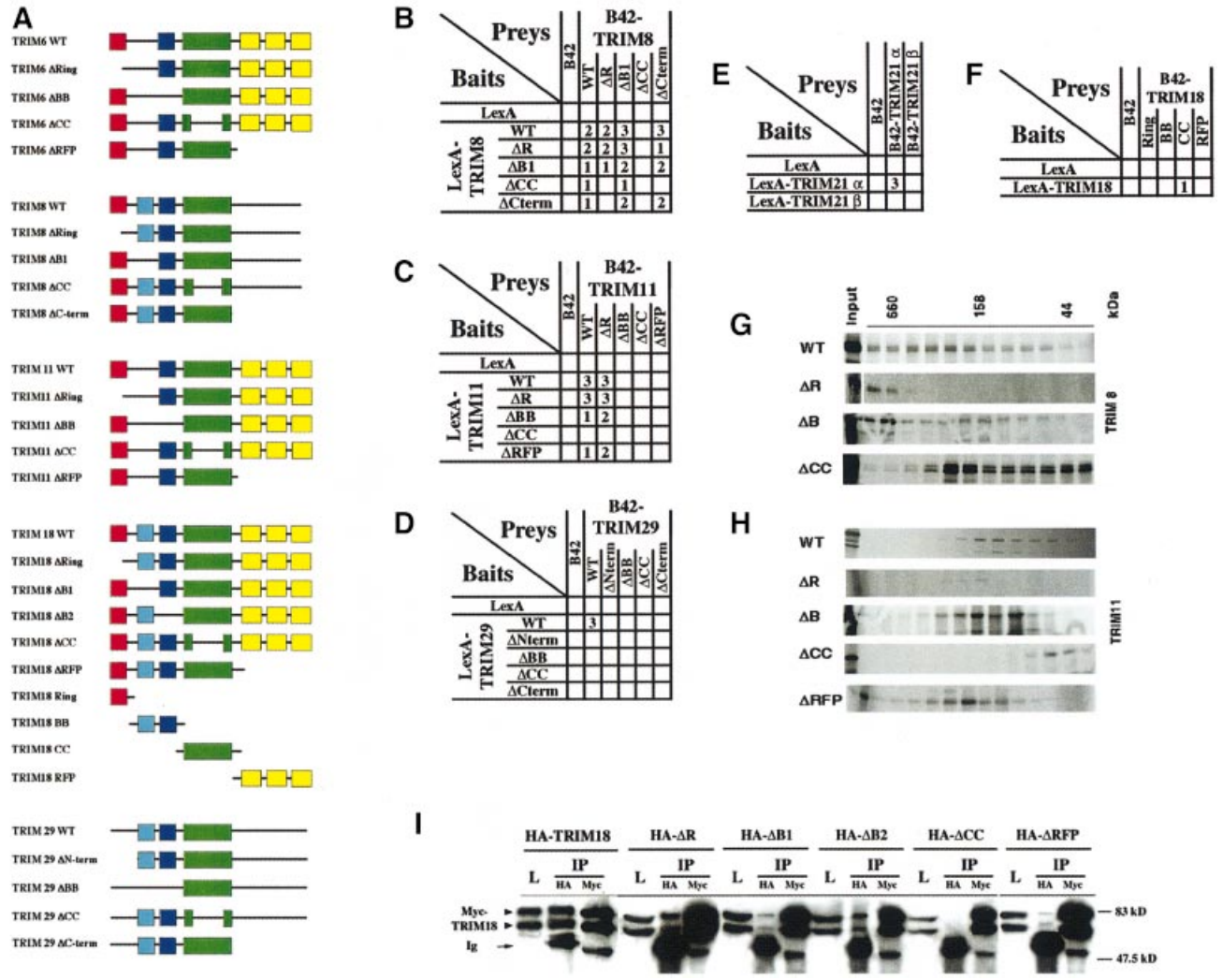


**Fig. 5.** Characterization of TRIM deletion mutants. (**A**) Schematic representation of the deletion mutants and the TRIM18 domains. The color coding is as defined in Figure 2A. (B–F) Interaction-mating assays between strains carrying TRIM8 (**B**), TRIM11 (**C**) and TRIM29 (**D**) deletion mutants, TRIM18 domains (**F**) and the naturally occurring TRIM21α and β isoforms (**E**). EGY42 bait strains containing plasmids that expressed LexA fusions were mated to EGY48 derivatives that contained B42 fusions. Numbers (1–3) indicate the degree of β-galactosidase activity on GAL plates. No activity was detected for the interaction represented by open squares. Please note that some residual binding is still apparent in the combinations TRIM8ΔCC/TRIM8WT and TRIMΔCC/TRIM8ΔB1. (G and H) Gel filtration of *in vitro* translated TRIM8 (**G**) and TRIM11 (**H**) deletion mutant proteins. The monomeric sizes are as follows. TRIM8: WT, 61 kDa; ΔR, 53 kDa; ΔB, 56 kDa; ΔCC, 50 kDa; and TRIM11: WT, 51 kDa; ΔR, 43 kDa; ΔB, 48 kDa; ΔCC, 40 kDa; ΔRFP, 35 kDa. (**I**) Co-immunoprecipitation experiments of HA-tagged TRIM18 mutants and Myc-tagged TRIM18 expressed in Cos7 cells.

function of all family members. Our scheme allowed us to show that a given structural motif, the TRIM, defines a family of proteins and a cellular function (compartmentalization), thereby allowing the assignment of a common function to homologous proteins.

Cells set apart specific functions even without the help of membranes, thus rendering the process dynamic and flexible to physiological changes. These functional compartments are defined by specific proteins and are found both in the nucleus and in the cytoplasm. Our data indicate that the TRIM-containing proteins may serve a fundamental role in defining such subcompartments. TRIM proteins present the expected features that one can hypothesize as being necessary to fulfill this task; triggered by homodimerization, they form high molecular weight complexes that identify subcellular niches. Consistently, PML (TRIM19), but not other proteins localizing within the PML nuclear bodies, is necessary for the correct constitution of this compartment (Ishov *et al*., 1999; Zhong *et al*., 1999b).

Formation of distinct cellular compartments by TRIM proteins is strictly dependent on the integrity of the TRIM. The CC domain is necessary and sufficient for homomultimerization, an essential step towards compartmentalization. Nevertheless, the other TRIM domains are also involved. Independent deletions of the R or BB regions result in the formation of different subcellular compartments. We hypothesize that TRIM domains, besides the CC region, provide the protein–protein interfaces for the recruitment of other proteins, to specify cellular compartments. Consistently, these domains were shown to contribute specific interaction moieties (Li *et al*., 1994; Bellini *et al*., 1995; Friedman *et al*., 1996; Hasegawa *et al*., 1996; Kim *et al*., 1996; Le Douarin *et al*., 1996; Moosmann *et al*., 1996; Nielsen *et al*., 1999; Pearson *et al*., 2000; Zhong *et al*., 2000a). Notably, the TRIM proteins,

**Table II.** Co-localizations of TRIM proteins with compartment-specific markers

| Name | Recycling endosomes[a] | Mitochondria[a] | | | Endocytic vesicles[a] | Clathrin-coated pits[a] | Golgi[a] | TGN[a] | Intermediate filaments[a] | Microtubules[a] | Actin[a] | PML bodies[a] | BRCA-1 bodies[a] | Coil bodies[a] | Spliceosomes[a] |
|---|---|---|---|---|---|---|---|---|---|---|---|---|---|---|---|
| | Transferrin[b] | Mito Tracker[b] | Cytochrome *c*[b] | mtHSP70[b] | AP2[b] | Clathrin[b] | Giantin[b] | Rab2[b] | Vimentin[b] | β-tubulin[b] | Phalloidin[b] | PMI[b] | BRCA-1[b] | p80 coilin[b] | SC35[b] |
| TRIM1 | | | | | | | | | | yes | | | | | |
| TRIM2 | | | | | | | | | no | no | no | | | | |
| TRIM3 | | | | | | | | | no | no | no | | | | |
| TRIM4 | no | | | no | no | no | no | no | | | | | | | |
| TRIM8 | | | | | | | | | | | | no | no | no | no |
| TRIM10 | no | | no | no | | | | | | | | | | | |
| TRIM12 | no | | | no | no | no | | | | | | no | | no | no |
| TRIM13 | no | | | | | | no | no | | | | | | | |
| TRIM14 | no | | | no | no | no | | | | | | | | | |
| TRIM18 | | | | | | | | | | yes | | | | | |
| TRIM19 | | | | | | | | | | | | yes | | | |
| TRIM21 | no | | no | no | | | | | | | | | | | |
| TRIM22 | no | no | | | | | | | | | | | | | |
| TRIM23 | no | | | no | no | no | | | | | | | | | |
| TRIM25 | no | | | no | no | no | no | no | | | | | | | |
| TRIM26 | no | | | no | no | no | no | no | | | | | | | |
| TRIM27 | no | | | | | | | | | | | | | | |
| TRIM29 | | | | | | | | | no | no | no | | | | |
| TRIM30 | no | no | | | | | | | | | | no | no | no | no |
| TRIM32 | no | no | | | | | | | | | | | | | |

[a]Tested subcellular compartment.
[b]Marker used in the colocalization experiments.

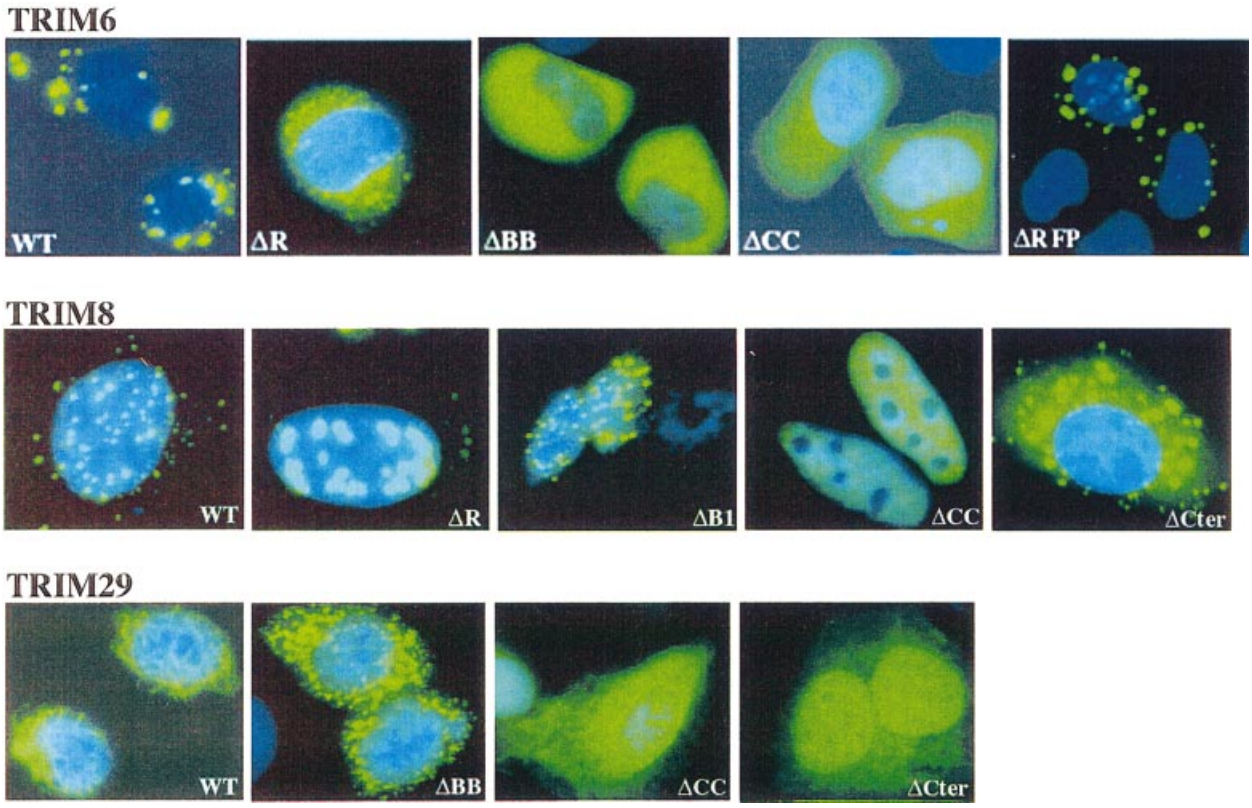


**Fig. 6.** Subcellular localization of TRIM6, 8 and 29 deletion mutants.

despite sequence and structural similarity, have no or little propensity to heterodimerize, have distinct patterns of expression and are not functionally interchangeable (Peng *et al*., 2000; this work), suggesting that they are single functional entities. Further studies are needed to clarify the role of TRIM proteins in compartmentalization and to identify other factors involved in this process.

## Materials and methods

### *Bioinformatics*

We created a reformatted, Blast-searchable version of the Unigene database (http://hercules.tigem.it/UNIBLAST/uniblast.html), which allowed us to identify EST matches. EST assembly and contig elongation were performed using 'The EST Extractor' tool (http://hercules.tigem.it/BLASTEXTRACT/estextract.html). We identified further members with recursive dbEST searches using the blastn/tblastn programs with the above isolated contigs as search keys. The cDNA clones were obtained from the IMAGE consortium and sequenced. Suitable libraries were screened to retrieve the full-length cDNA, when necessary. The low stringency conditions used for these library screenings allowed the isolation of additional members of the TRIM family.

### *cDNA clones and plasmids*

TRIM1: the full-length human and murine cDNAs were received from B.Franco. TRIM2: the human clone KIAA0517 was received from Takahiro Nagase, Kazusa DNA Research Institute. IMAGE clone 1380964 was used to screen a 15.5 d.p.c. mouse embryo cDNA library (Clontech) and to retrieve the full-length murine gene. TRIM3: IMAGE clone 1380964 was used to screen a 15.5 d.p.c. mouse embryo cDNA library (Clontech) and to retrieve the full-length murine gene. TRIM4: IMAGE clone 268148 was used to screen an NT2 cell cDNA library (Stratagene) and to retrieve the full-length gene. TRIM5: IMAGE clone 29808 was used as template. TRIM6: IMAGE clone 664116 was used as template. Murine probe was amplified from genomic DNA using the database sequence entry AA571501. TRIM7: IMAGE clone 925222 was used to screen a human skeletal muscle cDNA library (Clontech) and to retrieve the full-length gene. TRIM8: IMAGE clone 159487 was used to screen an NT2 cell cDNA library (Stratagene) and to retrieve the 3′ region of the gene and its 3′UTR. The full-length gene was reconstructed by *Pfu*I PCR amplification (Stratagene). TRIM9: KIAA0282, received from Kazusa DNA Research Institute, was used to screen a mature NT2 cell cDNA library (Stratagene) and to retrieve the full-length gene. TRIM10: IMAGE clones 424725 and 465060 were used as templates. TRIM11: IMAGE clone 554746 was used as template. TRIM12: IMAGE clone 463322 was used as template. TRIM13: IMAGE clones 294505 and 546282 were used as templates. TRIM14: clone KIAA0129 was received from Kazusa DNA Research Institute. TRIM19: human PML-3B open reading frame (ORF) was used as template. TRIM20: received from D.Kastner. TRIM21: received from E.Chan. TRIM22: received from N.Mechti. TRIM23: received from J.Moss and M.Vaughan. TRIM25: received from M.Muramatsu. TRIM26: received from T.Chu and J.Gruen. TRIM27: received from L.D.Etkin. TRIM28: received from E.O'Leary and J.V.Bonventre. TRIM30: received from H.Cantor. TRIM31: received from J.Iovanna and P.Pontarotti. TRIM32: received from R.A.Friedell. Plasmids allowing the expression of proteins fused to the GAL4 DNA binding domain, the Myc-tagged EGFP or the hemagglutinin (HA) tag were engineered from the pCDNA3+ vector (Invitrogen). These vectors were subsequently modified, together with the two-hybrid technology plasmids pEG202 and pJG4-5 (Gyuris *et al*., 1993), to present a common multiple cloning site. The full-length ORF of the TRIM genes was amplified with *Pfu*I polymerase (Promega or Stratagene) and cloned in the above vectors. Deletion mutants were created using the Quick-change mutagenesis kit (Stratagene) and appropriate oligonucleotides.

### *Mapping*

Oligonucleotide primers were designed based on the TRIM cDNA sequences and were used to screen the HGMP Genebridge 4 whole-genome radiation hybrid panels. Amplification results were submitted to the Whitehead Institute/MIT servers (http://www-genome.wi.mit.edu/cgi-bin/contig/rhmapper.pl). This server returned an MIT framework linked to the subject STS with a LOD score >3.0. The cytogenetic band location was inferred using both the MIT and the Genethon framework maps (http://www-genome.wi.mit.edu/cgi-bin/contig/phys_map and http://www.cephb.fr/quickmap.html). Primer sequences, amplification

conditions and results, together with mapping location, can be retrieved from our web site (www.tigem.it/TRIM).

### *Expression studies*

Northern blot filters from human adult or mouse tissues (Clontech) were hybridized with TRIM cDNA probes following the manufacturer's recommendations. Sense and antisense $^{35}$S-labeled riboprobes were transcribed using 3′UTR murine cDNA fragments corresponding to the different TRIM genes, cloned in pBS vector and linearized with appropriate restriction enzymes. Mouse embryo tissue sections were prepared and RNA *in situ* hybridization performed as described (Rugarli *et al*., 1993). In panels with the entire embryo, the white color represents the signal. In the micrographs showing sections after double exposure, the red color represents the *in situ* hybridization signal and the blue shows the nuclei stained with Hoechst 33258 dye.

### *Protein–protein interactions*

Interaction-mating techniques, an extension of the two-hybrid technology, are described. The bait plasmids express the cDNA fused directionally to the first 202 residues of LexA under the control of the constitutive ADH promoter. On the other hand, prey plasmids express cDNAs fused to the B42 activation domain, the SV40 T NLS and an HA tag under the control of the inducible GAL1 promoter. The pSH18-34 vector carrying the *lacZ* reporter gene driven by six LexA-operators was used. EGY48/EGY42 diploids for every pairwise combination were generated by mating (Gyuris *et al*., 1993; Finley and Brent, 1994; Reymond and Brent, 1995). The two-hybrid technology used in this report is based upon a transcriptional activation event that occurs in the nucleus. Hence, it can produce false negatives. For example, in this assay we did not detect the previously identified PML homo-interaction (Perez *et al*., 1993). Co-immunoprecipitation experiments were performed as described in Meroni *et al*. (2000). *In vitro* translated and labeled TRIM proteins were analyzed by size exclusion chromatography on a Superose 6 HR10/30 column (Pharmacia) equilibrated in 20 mM HEPES pH 7.5, 1% glycerol, 0.4 M KCl, 1 mM EDTA, 1 mM phenylmethylsulfonyl fluoride, 1 mM dithiothreitol. Fractions were collected and separated by SDS–PAGE. Proteins of known size were gel-filtrated to determine the molecular weight eluted in each fraction.

### *Subcellular localization*

HeLa and U2OS cells were transfected by calcium phosphate precipitation and the FUGENE (Boehringer Mannheim) procedure, to obtain low and high expression levels, respectively. EGFP fluorescence was detected on both living and fixed cells using epifluorescence (Olympus BX-60 equipped with 3CCD color camera Hamamatsu Photonics C5810) and confocal microscopy (Bio-Rad MRC-1024). Images were analyzed with the Adobe Photoshop software. A western blot analysis of transfected cells with anti-GFP monoclonal antibody (Clontech) was performed to control correct expression of the EGFP–TRIM fusion proteins. The fusion of EGFP to TRIM proteins has no influence on their localization, as shown by: (i) EGFP–TRIMX and HA–TRIMX co-localizations; (ii) EGFP–PML and endogenous PML co-localization; and (iii) EGFP–MID1 and endogenous MID1 co-localization. The following compartment-specific markers were used: monoclonal anti-PML (PGM3); monoclonal anti-Giantin (324450; Calbiochem); polyclonal anti-Rab2 (sc-307; Santa Cruz Biotechnology); monoclonal anti-AP2 (AP.6; Affinity Bioreagents); monoclonal anti-clathrin (X22; a kind gift from Werner Boll); monoclonal anti-mtHSP70 (MA3-028; Affinity Bioreagents); monoclonal anti-cytochrome *c* (65981A; PharMingen); monoclonal anti-BRCA-1 (AB-1; Calbiochem); monoclonal anti-p80 coilin (kindly provided by Angus Lamond); monoclonal anti-SC-35 (S4045; Sigma-Aldrich); monoclonal anti-β tubulin (KMX-1; Boehringer Mannheim); and monoclonal anti-vimentin (V9, sc-6260; Santa Cruz Biotechnology). Orange Red-conjugated MitoTracker, rhodamine-conjugated transferrin and rhodamine-conjugated phalloidin are from Molecular Probes. The internalization assay was performed as previously described (Lanzetti *et al*., 2000).

### *Accession numbers*

The human, murine and alternatively spliced TRIM cDNA isoforms are deposited in DDBJ/EMBL/GenBank with the following accession Nos: from AF220014 to AF220039, from AF220121 to AF220144, AF230976–77, from AF230401 to AF230412, from AF230385 to AF230400. Details can be accessed through www.tigem.it/TRIM.

## Acknowledgements

We would like to thank Maria Teresa Bassi, Roberta Carbone, Sara Droetto, Micaela Quarto, Anna Marchitiello, Ildo Nicoletti, Mirko Riboni, Gyorgy Simon, Sara Volorio and Massimo Zollo for core assistance and reagents. We are grateful to Giuseppe Borsani and Mario Traditi for the design of our web site, and to Pierre Colas, Christian Fankhauser, Elena Rugarli and Anne Simon for critical reading of the manuscript. This research was sponsored by a Telethon fellowship for foreigners in Italy to A.R., an AIRC grant and a March of Dimes grant to Ge.M., FIRC fellowships to Gi.M., L.L. and S.M., a Perugia University fellowship to L.L., an AIRC grant to P.G.P., a BIOMED2 CT97-BMH4-2284 EC grant (EURO-IMAGE) and a Merck Genome Research Institute grant to A.B., and by the Italian Telethon Foundation grant to TIGEM 1996–1999 and 2000–2002.

## References

Adams,M.D. *et al*. (2000) The genome sequence of *Drosophila melanogaster*. *Science*, **287**, 2185–2195.

Avela,K., Lipsanen-Nyman,M., Idanheimo,N., Seemanova,E., Rosengren,S., Makela,T.P., Perheentupa,J., Chapelle,A. and Lehesjoki,A.E. (2000) Gene encoding a new RING–B-box–coiled-coil protein is mutated in mulibrey nanism. *Nature Genet.*, **25**, 298–301.

Bellini,M., Lacroix,J.C. and Gall,J.G. (1995) A zinc-binding domain is required for targeting the maternal nuclear protein PwA33 to lampbrush chromosome loops. *J. Cell Biol.*, **131**, 563–570.

Blattner,F.R. *et al*. (1997) The complete genome sequence of *Escherichia coli* K-12. *Science*, **277**, 1453–1474.

Borden,K.L. (1998) RING fingers and B-boxes: zinc-binding protein–protein interaction domains. *Biochem. Cell Biol.*, **76**, 351–358.

Brent,R. (2000) Genomic biology. *Cell*, **100**, 169–183.

Buchner,G. *et al*. (1999) *MID2*, a homologue of the Opitz syndrome gene *MID1*: similarities in subcellular localization and differences in expression during development. *Hum. Mol. Genet.*, **8**, 1397–1407.

Cainarca,S., Messali,S., Ballabio,A. and Meroni,G. (1999) Functional characterization of the Opitz syndrome gene product (midin): evidence for homodimerization and association with microtubules throughout the cell cycle. *Hum. Mol. Genet.*, **8**, 1387–1396.

Cao,T., Borden,K.L., Freemont,P.S. and Etkin,L.D. (1997) Involvement of the rfp tripartite motif in protein–protein interactions and subcellular distribution. *J. Cell Sci.*, **110**, 1563–1571.

Cao,T., Duprez,E., Borden,K.L., Freemont,P.S. and Etkin,L.D. (1998) Ret finger protein is a normal component of PML nuclear bodies and interacts directly with PML. *J. Cell Sci.*, **111**, 1319–1329.

Dunham,I. *et al*. (1999) The DNA sequence of human chromosome 22. *Nature*, **402**, 489–495.

Dyck,J.A., Maul,G.G., Miller,W.H.,Jr, Chen,J.D., Kakizuka,A. and Evans,R.M. (1994) A novel macromolecular structure is a target of the promyelocyte-retinoic acid receptor oncoprotein. *Cell*, **76**, 333–343.

Finley,R.L.,Jr and Brent,R. (1994) Interaction mating reveals binary and ternary connections between *Drosophila* cell cycle regulators. *Proc. Natl Acad. Sci. USA*, **91**, 12980–12984.

Frank,D.J. and Roth,M.B. (1998) ncl-1 is required for the regulation of cell size and ribosomal RNA synthesis in *Caenorhabditis elegans*. *J. Cell Biol.*, **140**, 1321–1329.

Friedman,J.R., Fredericks,W.J., Jensen,D.E., Speicher,D.W., Huang, X.P., Neilson,E.G. and Rauscher,F.J.,III (1996) KAP-1, a novel corepressor for the highly conserved KRAB repression domain. *Genes Dev.*, **10**, 2067–2078.

Goffeau,A. *et al*. (1996) Life with 6000 genes. *Science*, **274**, 546, 563–567.

Grignani,F., Fagioli,M., Alcalay,M., Longo,L., Pandolfi,P.P., Donti,E., Biondi,A., Lo Coco,F. and Pelicci,P.G. (1994) Acute promyelocytic leukemia: from genetics to treatment. *Blood*, **83**, 10–25.

Grignani,F. *et al*. (1996) Effects on differentiation by the promyelocytic leukemia PML/RARα protein depend on the fusion of the PML protein dimerization and RARα DNA binding domains. *EMBO J.*, **15**, 4949–4958.

Grignani,F., Gelmetti,V., Fanelli,M., Rogaia,D., De Matteis,S., Ferrara,F.F., Bonci,D., Nervi,C. and Pelicci,P.G. (1999) Formation of PML/RARα high molecular weight nuclear complexes through the PML coiled-coil region is essential for the PML/RARα-mediated retinoic acid response. *Oncogene*, **18**, 6313–6321.

Gyuris,J., Golemis,E., Chertkov,H. and Brent,R. (1993) Cdi1, a human $G_1$ and S phase protein phosphatase that associates with Cdk2. *Cell*, **75**, 791–803.

Hasegawa,N., Iwashita,T., Asai,N., Murakami,H., Iwata,Y., Isomura,T., Goto,H., Hayakawa,T. and Takahashi,M. (1996) A RING finger motif regulates transforming activity of the *rfp/ret* fusion gene. *Biochem. Biophys. Res. Commun.*, **225**, 627–631.

Henry,J., Mather,I.H., McDermott,M.F. and Pontarotti,P. (1998) B30.2-like domain proteins: update and new insights into a rapidly expanding family of proteins. *Mol. Biol. Evol.*, **15**, 1696–1705.

Ishov,A.M., Sotnikov,A.G., Negorev,D., Vladimirova,O.V., Neff,N., Kamitani,T., Yeh,E.T., Strauss,J.F.,III and Maul,G.G. (1999) PML is critical for ND10 formation and recruits the PML-interacting protein daxx to this nuclear structure when modified by SUMO-1. *J. Cell Biol.*, **147**, 221–234.

Jacobson,R.H., Ladurner,A.G., King,D.S. and Tjian,R. (2000) Structure and function of a human TAFII250 double bromodomain module. *Science*, **288**, 1422–1425.

Kim,S.S., Chen,Y.M., O'Leary,E., Witzgall,R., Vidal,M. and Bonventre, J.V. (1996) A novel member of the RING finger family, KRIP-1, associates with the KRAB-A transcriptional repressor domain of zinc finger proteins. *Proc. Natl Acad. Sci. USA*, **93**, 15299–15304.

Lanzetti,L., Rybin,V., Malabarba,M.G., Christoforidis,S., Scita,G., Zerial,M. and Di Fiore,P.P. (2000) The Eps8 protein coordinates EGF receptor signalling through Rac and trafficking through Rab5. *Nature*, **408**, 374–377.

Le Douarin,B. *et al*. (1995) The N-terminal part of TIF1, a putative mediator of the ligand-dependent activation function (AF-2) of nuclear receptors, is fused to B-raf in the oncogenic protein T18. *EMBO J.*, **14**, 2020–2033.

Le Douarin,B., Nielsen,A.L., Garnier,J.M., Ichinose,H., Jeanmougin,F., Losson,R. and Chambon,P. (1996) A possible involvement of TIF1α and TIF1β in the epigenetic control of transcription by nuclear receptors. *EMBO J.*, **15**, 6701–6715.

Li,X., Shou,W., Kloc,M., Reddy,B.A. and Etkin,L.D. (1994) The association of *Xenopus* nuclear factor 7 with subcellular structures is dependent upon phosphorylation and specific domains. *Exp. Cell Res.*, **213**, 473–481.

Lupas,A. (1996) Coiled coils: new structures and new functions. *Trends Biochem. Sci.*, **21**, 375–382.

Martzen,M.R., McCraith,S.M., Spinelli,S.L., Torres,F.M., Fields,S., Grayhack,E.J. and Phizicky,E.M. (1999) A biochemical genomics approach for identifying genes by the activity of their products. *Science*, **286**, 1153–1155.

Meroni,G., Cairo,S., Merla,G., Messali,S., Brent,R., Ballabio,A. and Reymond,A. (2000) Mlx, a new Max-like bHLHZip family member: the center stage of a novel transcription factors regulatory pathway? *Oncogene*, **19**, 3266–3277.

Minucci,S. *et al*. (2000) Oligomerization of RAR and AML1 transcription factors as a novel mechanism of oncogenic activation. *Mol. Cell*, **5**, 811–820.

Moosmann,P., Georgiev,O., Le Douarin,B., Bourquin,J.P. and Schaffner,W. (1996) Transcriptional repression by RING finger protein TIF1β that interacts with the KRAB repressor domain of KOX1. *Nucleic Acids Res.*, **24**, 4859–4867.

Nielsen,A.L., Ortiz,J.A., You,J., Oulad-Abdelghani,M., Khechumian,R., Gansmuller,A., Chambon,P. and Losson,R. (1999) Interaction with members of the heterochromatin protein 1 (HP1) family and histone deacetylation are differentially involved in transcriptional silencing by members of the TIF1 family. *EMBO J.*, **18**, 6385–6395.

Pearson,M. *et al*. (2000) PML regulates p53 acetylation and premature senescence induced by oncogenic Ras. *Nature*, **406**, 207–210.

Peng,H., Begg,G.E., Schultz,D.C., Friedman,J.R., Jensen,D.E., Speicher,D.W. and Rauscher,F.J.,III (2000) Reconstitution of the KRAB–KAP-1 repressor complex: a model system for defining the molecular anatomy of RING–B box–coiled-coil domain-mediated protein–protein interactions. *J. Mol. Biol.*, **295**, 1139–1162.

Perez,A., Kastner,P., Sethi,S., Lutz,Y., Reibel,C. and Chambon,P. (1993) PMLRAR homodimers: distinct DNA binding properties and heteromeric interactions with RXR. *EMBO J.*, **12**, 3171–3182.

Quaderi,N.A. *et al*. (1997) Opitz G/BBB syndrome, a defect of midline development, is due to mutations in a new RING finger gene on Xp22. *Nature Genet.*, **17**, 285–291.

Quignon,F., De Bels,F., Koken,M., Feunteun,J., Ameisen,J.C. and de The,H. (1998) PML induces a novel caspase-independent death process. *Nature Genet.*, **20**, 259–265.

Reddy,B.A., Etkin,L.D. and Freemont,P.S. (1992) A novel zinc finger coiled-coil domain in a family of nuclear proteins. *Trends Biochem. Sci.*, **17**, 344–345.

Reymond,A. and Brent,R. (1995) p16 proteins from melanoma-prone families are deficient in binding to Cdk4. *Oncogene*, **11**, 1173–1178.

Ross-Macdonald,P. *et al*. (1999) Large-scale analysis of the yeast genome by transposon tagging and gene disruption. *Nature*, **402**, 413–418.

Rugarli,E.I., Lutz,B., Kuratani,S.C., Wawersik,S., Borsani,G., Ballabio, A. and Eichele,G. (1993) Expression pattern of the Kallmann syndrome gene in the olfactory system suggests a role in neuronal targeting. *Nature Genet.*, **4**, 19–26.

Schweiger,S. *et al*. (1999) The Opitz syndrome gene product, MID1, associates with microtubules. *Proc. Natl Acad. Sci. USA*, **96**, 2794–2799.

Shevchenko,A., Jensen,O.N., Podtelejnikov,A.V., Sagliocco,F., Wilm, M., Vorm,O., Mortensen,P., Boucherie,H. and Mann,M. (1996) Linking genome and proteome by mass spectrometry: large-scale identification of yeast proteins from two dimensional gels. *Proc. Natl Acad. Sci. USA*, **93**, 14440–14445.

Shou,W., Li,X., Wu,C., Cao,T., Kuang,J., Che,S. and Etkin,L.D. (1996) Finely tuned regulation of cytoplasmic retention of *Xenopus* nuclear factor 7 by phosphorylation of individual threonine residues. *Mol. Cell. Biol.*, **16**, 990–997.

Slack,F.J. and Ruvkun,G. (1998) A novel repeat domain that is often associated with RING finger and B-box motifs. *Trends Biochem. Sci.*, **23**, 474–475.

Slack,F.J., Basson,M., Liu,Z., Ambros,V., Horvitz,H.R. and Ruvkun,G. (2000) The lin-41 RBCC gene acts in the *C. elegans* heterochronic pathway between the let-7 regulatory RNA and the LIN-29 transcription factor. *Mol. Cell*, **5**, 659–669.

Takahashi,M., Inaguma,Y., Hiai,H. and Hirose,F. (1988) Developmentally regulated expression of a human 'finger'-containing gene encoded by the 5′ half of the *ret* transforming gene. *Mol. Cell. Biol.*, **8**, 1853–1856.

The *C. elegans* Sequencing Consortium (1998) Genome sequence of the nematode *C. elegans*: a platform for investigating biology. *Science*, **282**, 2012–2018.

The Chromosome 21 Mapping and Sequencing Consortium (2000) The DNA sequence of human chromosome 21. *Nature*, **405**, 311–319.

The French FMF Consortium (1997) A candidate gene for familial Mediterranean fever. *Nature Genet.*, **17**, 25–31.

The International FMF Consortium (1997) Ancient missense mutations in a new member of the RoRet gene family are likely to cause familial Mediterranean fever. *Cell*, **90**, 797–807.

Uetz,P. *et al*. (2000) A comprehensive analysis of protein–protein interactions in *Saccharomyces cerevisiae*. *Nature*, **403**, 623–627.

Venturini,L. *et al*. (1999) TIF1γ, a novel member of the transcriptional intermediary factor 1 family. *Oncogene*, **18**, 1209–1217.

Vitale,N., Moss,J. and Vaughan,M. (1996) ARD1, a 64-kDa bifunctional protein containing an 18-kDa GTP-binding ADP-ribosylation factor domain and a 46-kDa GTPase-activating domain. *Proc. Natl Acad. Sci. USA*, **93**, 1941–1944.

Walhout,A.J., Sordella,R., Lu,X., Hartley,J.L., Temple,G.F., Brasch, M.A., Thierry-Mieg,N. and Vidal,M. (2000) Protein interaction mapping in *C. elegans* using proteins involved in vulval development. *Science*, **287**, 116–122.

Wang,Z.G., Ruggero,D., Ronchetti,S., Zhong,S., Gaboli,M., Rivi,R. and Pandolfi,P.P. (1998) PML is essential for multiple apoptotic pathways. *Nature Genet.*, **20**, 266–272.

Zhong,S., Delva,L., Rachez,C., Cenciarelli,C., Gandini,D., Zhang,H., Kalantry,S., Freedman,L.P. and Pandolfi,P.P. (1999a) A RA-dependent, tumour-growth suppressive transcription complex is the target of the PML-RARα and T18 oncoproteins. *Nature Genet.*, **23**, 287–295.

Zhong,S., Hu,P., Ye,T.Z., Stan,R., Ellis,N.A. and Pandolfi,P.P. (1999b) A role for PML and the nuclear body in genomic stability. *Oncogene*, **18**, 7941–7947.

Zhong,S., Muller,S., Ronchetti,S., Freemont,P.S., Dejean,A. and Pandolfi,P.P. (2000a) Role of SUMO-1-modified PML in nuclear body formation. *Blood*, **95**, 2748–2752.

Zhong,S., Salomoni,P. and Pandolfi,P.P. (2000b) The transcriptional role of PML and the nuclear body. *Nature Cell Biol.*, **2**, E85–E90.

*Received October 26, 2000; revised March 8, 2001; accepted March 14, 2001*